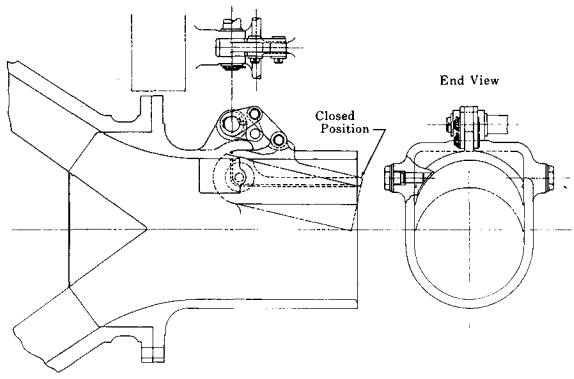

Fig. 21 Variable-geometry nozzle.

Waterjet nozzle designs are, for the most part, simple low-loss, fixed-area, converging nozzles. Their performance is depreciated seriously only when the flow from the pump stator contains appreciable rotational vectors or swirl, which is intensified by the nozzle contraction and can choke the pump flow.

Variable-area nozzles for waterjets are needed for vessels with a widely varying speed range, and when the inlet ram pressure is a significant portion of the system pressure. Under these conditions, changes in vessel speed cause significant changes in pump flow and tend to drive the unit into off-design conditions. By varying the nozzle area, the pump flow can be adjusted so that the pump operates at best efficiency. Figure 19 shows the effect of variable-area nozzles on thrust for a ship designed for 70 knots when it is operating at higher speeds. At 100 knots, the variable nozzle design gives 15% more thrust than the fixed nozzle. Figure 20 is a typical pump map that shows the extent of overflow and efficiency change at a 50% vessel overspeed. The variable-area nozzle can correct this overflow and adjust the jet velocity ratio to its optimum value. Mechanically, such nozzles are relatively straightforward designs. Figure 21 shows a variable geometry nozzle. Many other schemes are possible.

References

[1] Arcand, L., "Waterjet Propulsion for Small Craft," Small Craft Hydrodynamics Southeast Section Meeting, May 27, 1966, Society of Naval Architects and Marine Engineers.

[2] Traksel, J. and Beck, W. E., "Waterjet Propulsion for Marine Vehicles," Paper 65-245, 1965, AIAA; also *Journal of Aircraft*, Vol. 3, No. 2, March–April 1966, pp. 167–173.

[3] Wislicenus, G. F., "Hydrodynamics and Propulsion of Submerged Bodies," *ARS Journal*, Vol. 30, No. 12, Dec. 1960.

[4] Mossman, E. A. and Randall, L. M., "An Experimental Investigation of the Design Variables for NACA Submerged Duct Entrances," RMA7130, Jan. 1948, NACA.

[5] Hoerner, S. F., *Fluid Dynamic Drag*, Hoerner, Midland Park, N. J., 1958, pp. 9–16.

[6] Thurston, S. and Evanvar, M. S., "Efficiency of a Propulsor on a Body of Revolution Inducting Boundary-Layer Fluid," *Journal of Aircraft*, Vol. 3, No. 3, May 1966, pp. 270–277.

[7] Gearhart, W. S. and Henderson, R. E., "Selection of a Propulsor for a Submersible System," Paper 65-232, 1965, AIAA; also *Journal of Aircraft*, Vol. 3, No. 1, Jan.–Feb. 1966, pp. 84–90.

JANUARY 1968 J. HYDRONAUTICS VOL. 2, NO. 1

Prediction of the Seakeeping Characteristics of Hydrofoil Ships

IRVING A. HIRSCH*
The Boeing Company, Seattle, Wash.

Three methods for predicting the foilborne seakeeping characteristics of fully submerged-foil hydrofoil ships are presented. Each method uses an analog computer simulation of a hydrofoil ship and its sea-state environment. The first method, applicable only to regular waves, uses a sinusoidal representation of the sea. The second method is based on a statistical description of the wave height and orbital particle velocity. In the third method, the simulated ship's response to selected sinusoidal waves is combined with the spectral density function of wave height to yield a prediction of the ship's seakeeping characteristics in irregular waves. Each of the three methods has been used successfully in designing and evaluating automatic control systems for hydrofoil ships. Representative samples of seakeeping predictions obtained by each method are presented.

Introduction

HIGH-SPEED operation with good seakeeping characteristics forms the basic justification for the submerged-foil hydrofoil ship. The ability to predict the behavior of the hydrofoil ship in a given sea state is an important element in the design of the ship, and specifically, in the design and evaluation of the ship's automatic control system. The purpose of this paper is to describe three analytical techniques that can be used in predicting the foilborne seakeeping characteristics of submerged-foil hydrofoil ships.

Each of the methods presented uses a comprehensive electronic analog computer simulation of the hydrofoil ship and of the sea-state environment. In the simulation, the wave height and wave orbital particle velocity are represented. Both of these wave properties act as disturbances on the simulated ship. A simulated 70-ton preliminary-design hydrofoil ship is used in this paper as a basis for the presentation of computer predictions.

Presented as Paper 67-352 at the AIAA/SNAME Advanced Marine Vehicles Meeting, Norfolk, Va., May 22–24, 1967; submitted June 8, 1967; revision received October 23, 1967. The author wishes to thank J. D. Burroughs, R. M. Hubbard, and J. J. Jamieson for their helpful comments in preparing this paper.

* Associate Research Engineer, Controls Staff, Advanced Marine Systems, Aerospace Group.

Computer Model

Attempts to predict the seakeeping characteristics of large hydrofoil ships based on the performance of smaller craft or models have been relatively unsuccessful because of the difficulties of adequately representing the inertial properties and dynamic characteristics of the active control system of full-scale ships. The use of the analog computer as the mathematical model permits adequate representation of the inertial properties and the control system of a full-scale ship. The computer model that has been used for the example of this paper has six degrees of freedom (that is, pitch, heave, surge, roll, yaw, and sway) with continuously variable speed and hull height above the water. For predicting behavior in rough seas, the simulation of a hydrofoil ship must reflect realistically the properties of the actual ship in all essential details. That is, accurate values must be known for ship weight, moments of inertia, and pertinent dimensions. The hydrodynamic characteristics of the foil-strut assemblies must be based on thorough model tests with results adjusted to include full-scale effects where appropriate. The lift, drag, and side forces developed by the foil-strut assemblies must be represented properly in response to changes in foil submergence, craft forward speed, foil angle of attack, strut angle of attack, and control surface deflections. The dynamic properties of the automatic control system must be represented in detail, including the characteristics of the control electronics, electrohydraulic servo actuators, and sensors. Typical sensors on a hydrofoil ship include a vertical gyroscope, a yaw-rate gyroscope, one or more accelerometers, and a height sensor mounted at the bow of the ship. Inherent control system limits, such as exist for control surface rate and position, must also be included.

Sea-state effects act on the simulated ship as disturbance functions. For the foilborne ship considered here, the disturbances act at each foil-strut location and at the height sensor. The sea profile at the height sensor generates an error signal in the control system electronics which represents a departure from the commanded height. This error signal is processed by the automatic control system which, in turn, delivers a command to change the position of the control surfaces.

One effect of the sea on the foil-strut assemblies is to generate a change in submergence at each assembly. This change in submergence affects the lift, drag, and side forces. In addition, the simulated water orbital particle velocity affects the effective angle of attack of the foils and local sideslip angle of the struts. This change in angle of attack and sideslip angle in turn affects the lift, drag, and side forces.

Sinusoidal Sea

The simplest method of representing a seaway on the analog computer is to assume that the wave profile can be described by a long-crested sinusoidal wave having a specified wave height and length. Although this technique of representing the sea is the least realistic method to be discussed, very useful information is obtained nevertheless. The instantaneous wave height for the sinusoidal or regular wave can be expressed as

$$h = (H/2)\sin(\omega t) \tag{1}$$

where

h = instantaneous wave height above the mean water level
H = distance from trough to crest of a wave
t = time
ω = wave frequency in rad/sec

Saunders[1] has compiled some basic wave assumptions that can be made for regular waves. He has shown that the velocity of wave propagation, more commonly called wave celerity, can be calculated from the following relationship:

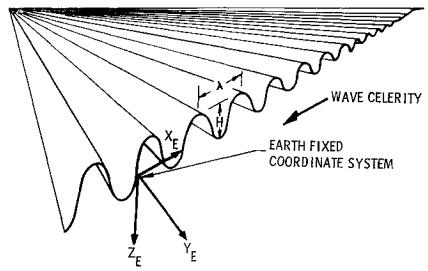

Fig. 1a Sinusoidal water surface.

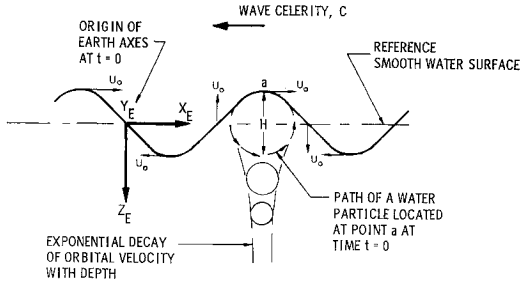

Fig. 1b Orbital particle velocity characteristics.

$$C = (g\lambda/2\pi)^{1/2} \tag{2}$$

where

λ = wave length g = acceleration due to gravity

C = wave celerity π = numeric const (3.1415 . . .)

Saunders has also shown that the vertical component w of the tangential orbital velocity u_o is the time derivative of the wave height. This can be expressed as

$$w = dh/dt = (\omega H/2)\cos(\omega t) = u_o \cos(\omega t) \tag{3}$$

The particle orbit is usually elliptical in nature. However, if the water depth is large compared to the wave length, the orbit can be assumed to be circular. A circular particle motion is assumed here. The horizontal orbital particle velocity component u has a phase-quadrature relationship with the vertical component. By choosing the direction of wave travel as negative, the horizontal component lags the vertical component by a phase angle of 90 deg. This is expressed as

$$u = u_o \sin(\omega t) \tag{4}$$

Saunders has also shown that the tangential orbital velocity decays exponentially with depth and can be expressed by

$$u_{o\text{decay}} = u_o \exp(-2\pi S/\lambda) \tag{5}$$

where S is the distance below the surface.

A sinusoidal water surface is depicted in Fig. 1a. The earth coordinate axes are X_E, Y_E, and Z_E and are shown to establish a reference system. The orbital particle velocity characteristics of a sinusoidal wave are shown in Fig. 1b. Note the exponential decay of the orbital velocity with depth.

The equations developed thus far represent the sea at a fixed point with respect to the earth. These equations must be modified to account for craft speed, craft heading, and spatially separated foil locations. From an observation point moving with a forward velocity U_o, the water surface appears as

$$Z_{EW} = (H/2)\sin[(2\pi/\lambda)(C + V_E)t] \tag{6}$$

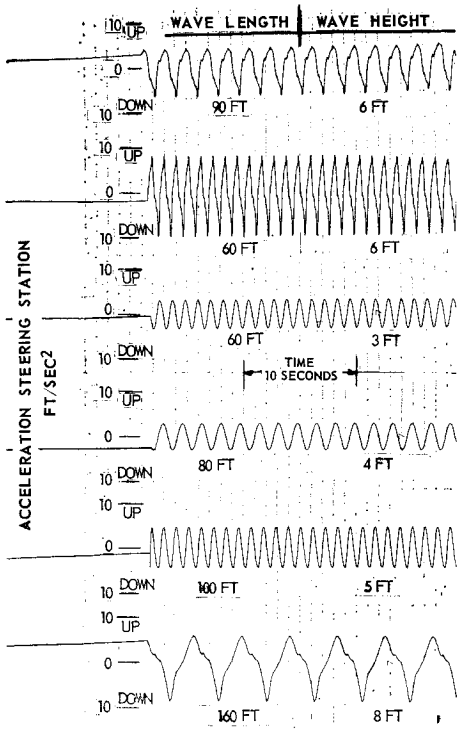

Fig. 2 Acceleration time responses in sinusoidal waves.

where

Z_{EW} = distance from the coordinate system origin to the water surface (Fig. 1a)
V_E = craft velocity relative to the sea

For most operations it can be assumed

$$V_E = U_o \cos\psi \tag{7}$$

where

U_o = craft forward equilibrium speed
ψ = craft heading angle ($\psi = 0$ deg corresponds to a head-sea condition. $\psi = 180$ deg corresponds to a following sea.)

The water surface is observed from the height sensor and foil locations that are fixed relative to one another but are moving relative to the Earth axes coordinate system. It is necessary to introduce phase lags that describe the height of the water surface at these points. The phase lags are determined by craft geometry and heading angle. When these phase lags are included, the equations for water surface heights, as seen from a craft maneuvering on a sine sea, can be expressed as

$$Z_{EW_i} = \frac{H}{2} \sin\left\{\frac{2\pi}{\lambda}[(C + V_E)t + l_{X_i}\cos\psi - l_{Y_i}\sin\psi]\right\} \tag{8}$$

where

Z_{EW_i} = instantaneous wave height at the ith foil measured in Earth axes from the reference mean water surface
l_{X_i} = distance from the height sensor along the X axis to the ith foil
l_{Y_i} = distance from the craft centerline along the Y axis to the ith foil (starboard is positive)

In a manner similar to that used in determining the wave height at each foil, the orbital particle velocity in Earth axes can be expressed as

$$U_{EW_i} = u_o \sin\{(2\pi/\lambda)[(C + V_E)t + l_{X_i}\cos\psi - l_{Y_i}\sin\psi]\} \exp(-2\pi S_i/\lambda) \tag{9}$$

and

$$W_{EW_i} = u_o \cos\{(2\pi/\lambda)[(C + V_E)t + l_{X_i}\cos\psi - l_{Y_i}\sin\psi]\} \exp(-2\pi S_i/\lambda) \tag{10}$$

where

U_{EW_i}, W_{EW_i} = components of water orbital particle velocity of Earth X axis and Z axis, respectively, at the ith foil
S_i = submerged distance of the ith foil

The instantaneous wave heights described in Eqs. (6) and (8) and the instantaneous orbital particle velocity components described in Eqs. (9) and (10) are simulated on the analog computer. These equations are then resolved into the craft coordinate system.

To evaluate properly a hydrofoil ship in regular waves it is necessary to operate the ship in waves of various heights and lengths. Time-history responses of the vertical acceleration at the steering station to a variety of wave heights and lengths are shown in Fig. 2. These responses were taken for a preliminary-design, 70-ton hydrofoil ship operating at 40 knots in a following sea. From the figure it is noted that the nonlinearities in the force characteristics of the hydrofoil ship are evidenced by the distorted sinusoidal response. However, it can be seen that the responses are approximately linear in the lower sea states, if the ratio of wave length-to-height is large (greater than 20 to 1).

The major advantage of the sine-sea method for predicting seakeeping over the other methods to be discussed is the ability to represent a hydrofoil ship performing a continuous 360-deg turn. An analog computer time-history trace of various ship responses for turning in regular waves with a fixed helm command is shown in Fig. 3. The wave height is 5 ft and the length is 75 ft. The forward foil depth response shows the craft to be maintaining a near-platforming attitude in head and following seas where the encountered frequencies are relatively high. However, the craft contours the lower-frequency waves around the beam and quartering seas. The initial starboard roll angle is due to the fact that the ship turns in a banked turn mode. The rudder angle varies in a

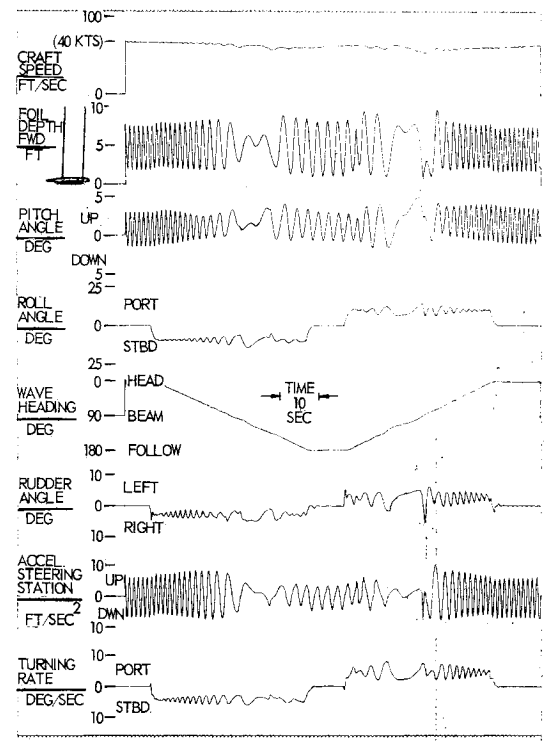

Fig. 3 A hydrofoil ship turning in sinusoidal waves.

turn even though there is a fixed helm. This is a result of the yaw rate feedback signal to the rudder. It has been found that some ship designs have considerable difficulty negotiating headings between a beam and a quartering sea. A yaw rate feedback signal to the rudder has eliminated most of this difficulty. Note that for this particular sea state the acceleration time response shows that the peak-to-peak vertical acceleration is significantly less in a following sea than in a head sea.

Random Sea

Observations readily verify that a seaway in nature is composed of numerous wave heights and lengths. Neumann[2] and others[3,4] have formulated analytic expressions for ocean waves based on statistical concepts of continuous random events. A Neumann wave spectrum for a fully arisen, long-crested sea can be expressed as

$$[H(\omega)]^2 = (C_1/\omega^6) \exp[-2(g/U_w\omega)]^2 \qquad (11)$$

where

$[H(\omega)]^2$ = spectral density of wave height
C_1 = empirically determined const = 51.6 ft^2/sec^5
U_w = wind velocity

Equation (11) provides a basis for simulating the wave height properties of a random sea.

Also required in the simulation are the spectra for the components of orbital velocity. In a sinusoidal sea the vertical component of orbital particle velocity is the time derivative of the wave height. It is assumed that a statistical sea is an infinite summation of sinusoids with a Gaussian distribution. Therefore, it can be assumed that the vertical orbital particle velocity is the time derivative of the wave height for the statistical sea. From random process theory,[5] it is known that if two functions are related by a time derivative, such as is the case with the vertical orbital velocity and wave height, their spectra are related by

$$[W(\omega)]^2 = \omega^2[H(\omega)]^2 \qquad (12)$$

where $[W(\omega)]^2$ = spectral density of the vertical component of orbital velocity. Note that there is no explicit phase relationship between the individual frequency components of vertical orbital velocity. However, each vertical orbital particle component at a particular frequency has a definite phase relationship (90-deg lead) with the component of wave height at that frequency. This phase relationship must be preserved in the simulation.

The horizontal component of orbital particle velocity $[U(\omega)]^2$ has the same spectral density characteristics as the vertical component of orbital velocity. However, each frequency component of $[U(\omega)]^2$ lags the corresponding component of $[W(\omega)]^2$ by 90 deg at each frequency. This relationship must also be observed in the simulation.

The generated spectra are only valid for a stationary point in space. These spectra must be transformed to account for craft speed and heading. To preserve the energy of the spectra in a transformation, it can be shown that the transformed spectral density curves can be expressed as

$$[H(\omega_e)]^2 = \frac{[H(\omega)]^2}{|1 + (2U_o\omega/g) \cos\psi|} \qquad (13)$$

and

$$[W(\omega_e)]^2 = [U(\omega_e)]^2 = \omega^2[H(\omega_e)]^2 \qquad (14)$$

where

$[H(\omega_e)]^2$ = transformed spectral density of wave height
$[W(\omega_e)]^2$ = transformed spectral density of vertical component of orbital velocity
$[U(\omega_e)]^2$ = transformed spectral density of horizontal component of orbital velocity

The procedure that has been selected to generate a statistical sea on the analog computer is based on "shaping" a continuous white Gaussian noise signal with electronic filters and obtaining a continuous spectrum. This method is considered superior to using a line spectrum in which a finite sum of sinusoids is assumed. It is possible to inadvertently omit resonant frequencies of the craft when a line spectrum is assumed. To help understand the basis for generating a continuous spectrum, consider the following diagram:

$$S_X(\omega) \rightarrow \boxed{G(j\omega)} \rightarrow S_Y(\omega)$$

in which

$S_X(\omega)$, $S_Y(\omega)$ = input and output spectral densities, respectively
$G(j\omega)$ = transfer function of a linear filter

Because $G(j\omega)$ is a linear transfer function, the following is true:

$$S_Y(\omega) = |G(j\omega)|^2 S_X(\omega) \qquad (15)$$

By making $S_X(\omega)$ white Gaussian noise with a noise level of 1.0 ft^2/rad/sec, $S_Y(\omega)$ will be numerically equal to $|G(j\omega)|^2$. This implies that the output spectral density at each frequency will be equal to the square of the magnitude of the filter transfer function at that frequency. The converse of this is used in designing filters. That is, the filter transfer function is simply the square root of the desired output spectrum at each frequency.

A digital computer program based on an extremum-seeking technique has been developed to design the necessary filters. The digital computer program is capable of determining the necessary transfer functions with the proper amplitude and phase relationships. Separate filter transfer functions are needed for the wave height at the height sensor and at each foil. Filters are also required for the components of orbital particle velocity at each foil. A total of 10 filters is required theoretically to represent the sea.

To reduce the required number of filters, an approximation is made. It is assumed that the sea is a position-stationary process relative to the height sensor and the foils. As a result of this approximation, the foils "see" the same sea as the height sensor, suitably displaced in time. The time delay is simply a function of craft speed, craft heading, wave celerity, and foil distance from the height sensors. This relationship is approximately

$$t_i = (l_{Xi} \cos\psi - l_{Yi} \sin\psi)/(U_o \cos\psi + C) \qquad (16)$$

Predicted hydrofoil-ship responses are obtained by "flying" the hydrofoil ship in the realistic sea. Time histories of craft responses in a random sea are shown in Fig. 4. These responses were taken for the 70-ton hydrofoil ship operating in a head sea, traveling at 40 knots in Sea State 4. Observe that in no case do the peak accelerations at the steering station exceed 0.25 g.

One of the more useful methods of presenting statistical data is in the form of spectral density plots. The procedure for obtaining this type of prediction involves the recording of a time-history sample of the desired response on magnetic tape and then processing of the tape through an electronic spectrum-analysis machine.

An electronically measured spectral density plot of a simulated Neumann wave height spectrum is shown in Fig. 5. The simulated spectrum is that of upper Sea State 4 for a craft traveling 40 knots in a head sea. The predicted acceleration response spectrum for the craft operating in this sea state is shown in Fig. 6. The root mean square (rms) acceleration is 3.54 ft/sec^2 centered about 0.4 cycle per second (cps). Note that the predicted acceleration spectrum peaks at certain frequencies. If a line wave height spectrum were used

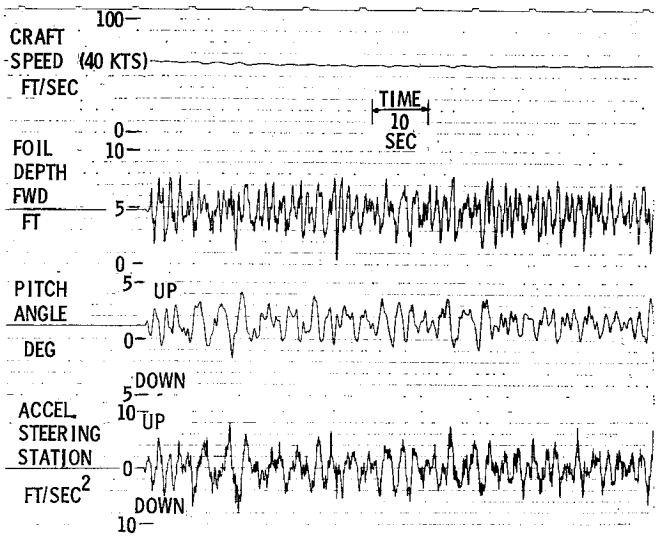

Fig. 4 Hydrofoil ship time responses in a random sea.

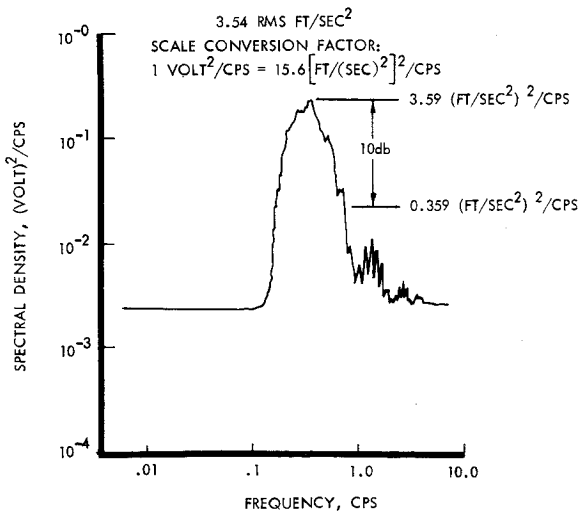

Fig. 6 Vertical acceleration spectrum at the steering station.

rather than the continuous spectrum, these peaks could have been undetected.

An electronically measured craft pitch angle spectrum is shown in Fig. 7. The rms value pitch angle is 1.04 deg and the spectrum is centered about 0.25 cps. Again, note that peaking occurs at various frequencies.

Linear Superposition Technique

R. P. Bernicker[6,7] has shown that hydrofoil craft motions can be predicted in a random sea from knowledge of hydrofoil-craft responses in a regular sea. Bernicker conducted his study in a water tow tank with a model of a surface-piercing hydrofoil craft. He showed that the technique was valid for a nonventilated foil system and for a fully ventilated foil system. The same technique can be shown to be applicable to a fully submerged-foil hydrofoil for which the analog computer acts as the model.

The technique that is used to predict craft response in a random sea is a linear analysis technique for which a closed-loop dynamic transfer function must be determined between the wave height and the ship responses. On the basis of the theory of linear superposition, the output response spectrum is the product of the value of the wave height spectral density at each discrete frequency and the square of the absolute value of the transfer function at the corresponding frequency. The successful application of this method depends on nonlinear effects being minor.

Experiments were conducted on the analog computer to determine under what conditions the assumption of linearity was valid. The analog simulation of the hydrofoil ship involves many nonlinear elements. In spite of this, for small amplitude, long period waves the ship responses were quite linear. For steep waves and for large amplitude waves of the order of the strut length, the nonlinearities became more pronounced and the validity of the method became questionable.

Figure 8 shows the measured response spectrum of after vertical acceleration for an alternate hydrofoil-ship design. This continuous spectrum was obtained in response to shaped white noise as previously discussed. Also shown are predicted response spectrum points that were calculated by this linear superposition technique. Predicted points at frequencies of below 1.0 cps show exceptionally good correlation. The confidence of predicted points greater than 1.0 cps may be questionable because this would represent steep waves which produce nonlinear operations. However, because all predicted points fall within ± 3.0 db of actual data, the correlation is considered to be good.

Figure 9 shows the response spectrum of forward vertical acceleration for the same craft and sea. The time history of the forward vertical acceleration in the simulated random sea showed that the forward foil broached on occasion. Broaching induces highly nonlinear effects and the linear

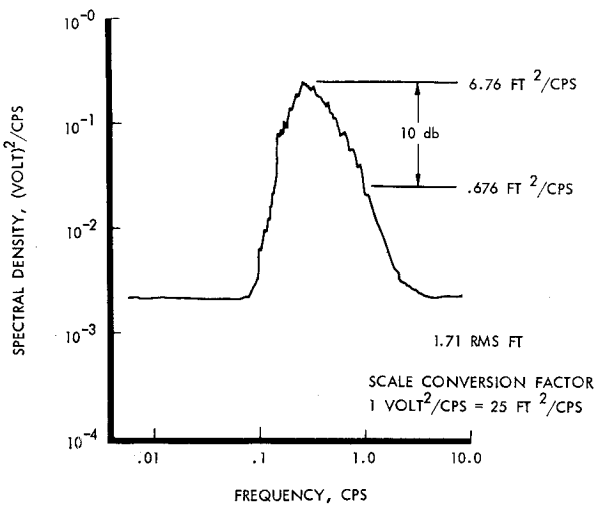

Fig. 5 Wave height spectrum.

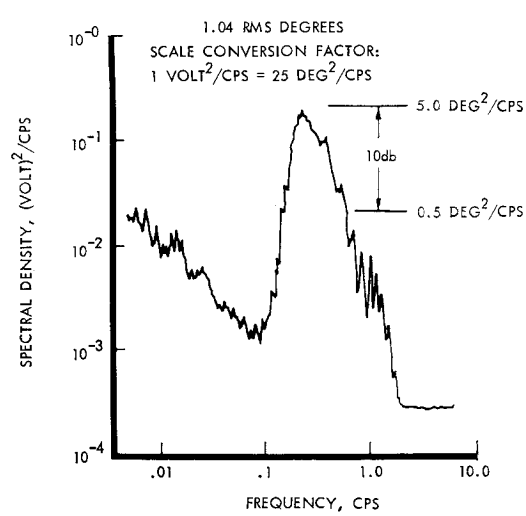

Fig. 7 Craft pitch angle spectrum.

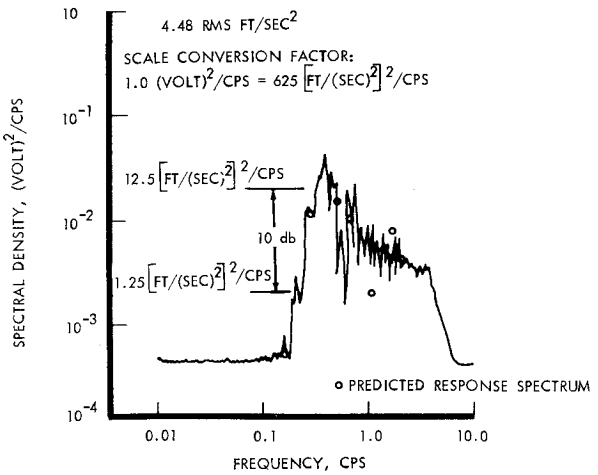

Fig. 8 Aft vertical acceleration spectrum.

analysis must be used with caution. Foil broaching would appear as narrow-band square-wave pulses to the spectrum analysis equipment and the spectral density plot of square pulses appears as very low-frequency power. Forward foil broaching will affect all craft responses under investigation. However, it is reasonable to assume that the forward vertical acceleration will be affected significantly more than the other responses. The lowest prediction point in Fig. 9 is 14 db in error due to foil broaching. All other predicted points are within ± 3.0 db of actual data.

Figure 10 shows a continuous spectrum of craft-pitch angle compared with points on the spectrum predicted by superposition. All predicted points show good correlation with continuous data. However, a technique limitation can be observed from the figure. The actual spectrum peaks sharply between 0.3 and 0.5 cps. No predicted point was chosen in this band. Because the method is only valid at discrete frequencies, there would be no way of knowing that peaking would occur in this band unless a point had been chosen in it.

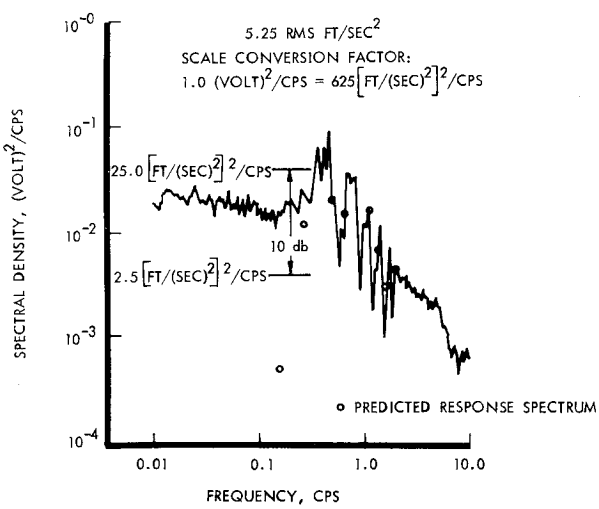

Fig. 9 Forward vertical acceleration spectrum.

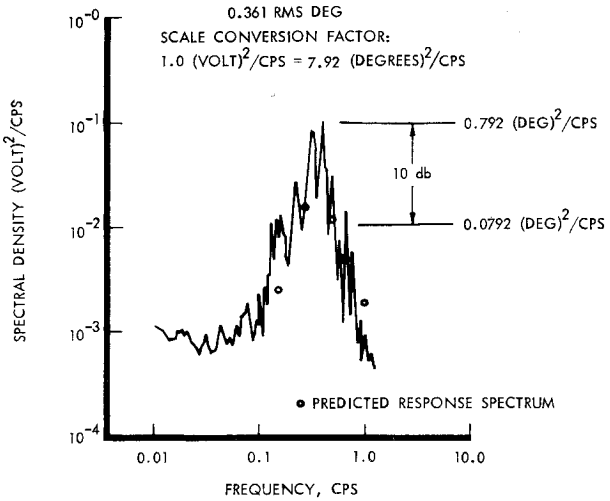

Fig. 10 Pitch angle spectrum.

Concluding Remarks

The first prediction method that was discussed was based on the sinusoidal sea. While this technique was the least realistic method, valuable control system design information can be obtained from it. The hydrofoil ship can be evaluated over a full range of wave heights and wave lengths. Craft performance can be obtained in the sinusoidal sea either by flying the ship at a fixed heading or by performing turns.

The second method discussed was based on the random sea. This technique makes use of filters to "shape" a continuous white Gaussian noise signal. By the proper choice of filters the wave height spectrum and particle velocity spectra are obtained. Spectral density plots were used to present craft performance data.

The final method was a linear superposition technique in which a transfer function was obtained. The transfer function was then combined with the spectral density function of the wave height to give a prediction of the hydrofoil's seakeeping characteristics.

References

[1] Saunders, H. E., *Hydrodynamics in Ship Design—Vol. I*, The Society of Naval Architects and Marine Engineers, New York, 1957.

[2] Neumann, G., "On Ocean Wave Spectra and a New Method of Forecasting Wind-Generated Seas" Technical Memo. 43, 1953, Beach Erosion Board, Corps of Engineers.

[3] Pierson, W. J., Jr. and St. Denis, M., "On the Motions of Ships in Confused Seas," *Transactions of the Society of Naval Architects and Marine Engineers*, Vol. 61, 1953.

[4] Bunting, D. C., "Wave Hindcase Project North Atlantic Ocean," Jan. 1966, U.S. Naval Oceanographic Office, Washington, D.C.

[5] Davenport, W. B., Jr. and Root, W. L., *An Introduction to the Theory of Random Signals and Noise*, McGraw-Hill, New York, 1958.

[6] Bernicker, R. P., "Hydrofoil Motions in Irregular Seas," Rept. 909, Nov. 1962, Davidson Lab.

[7] Bernicker, R. P., "Heaving and Pitching Motions of Superventilated Hydrofoil Craft in Irregular Seas," Rept. 958, June 1963, Davidson Lab.